AGU PUBLICATIONS

JGR

Journal of Geophysical Research: Biogeosciences

RESEARCH ARTICLE
10.1002/2015JG002952

In situ characterization of forest litter using ground-penetrating radar

Frédéric André[1], François Jonard[1,2], Mathieu Jonard[1], and Sébastien Lambot[1]

[1]Earth and Life Institute, Université catholique de Louvain, Louvain-la-Neuve, Belgium, [2]Institute of Bio- and Geosciences, Forschungszentrum Jülich GmbH, Jülich, Germany

Key Points:
- Ultrawideband radar data were acquired *in situ* above different forest litters
- Litter constitutive properties were estimated using full-wave inverse modeling
- Litter thickness, permittivity, and electrical conductivity were well retrieved

Correspondence to:
F. André,
frederic.andre@uclouvain.be

Citation:
André, F., F. Jonard, M. Jonard, and S. Lambot (2016), *In situ* characterization of forest litter using ground-penetrating radar, *J. Geophys. Res. Biogeosci.*, *121*, 879–894, doi:10.1002/2015JG002952.

Received 10 FEB 2015
Accepted 24 FEB 2016
Accepted article online 27 FEB 2016
Published online 21 MAR 2016

Abstract Decomposing litter accumulated on the soil surface in forests plays a major role in several ecosystem processes; its detailed characterization is therefore essential for thorough understanding of ecosystem functioning. In addition, litter is known to affect remote sensing radar data over forested areas and their proper processing requires accurate quantification of litter scattering properties. In the present study, ultrawideband (0.8–2.2 GHz) ground-penetrating radar (GPR) data were collected *in situ* for a wide range of litter types to investigate the potential of the technique to reconstruct litter horizons in undisturbed natural conditions. Radar data were processed resorting to full-wave inversion. Good agreement was generally found between estimated and measured litter layer thicknesses, with root-mean-square error values around 1 cm for recently fallen litter (OL layer) and around 2 cm for fragmented litter in partial decomposition (OF layer) and total litter (OL + OF). Nevertheless, significant correlations between estimated and measured thicknesses were found for total litter only. Inaccuracies in the reconstruction of the individual litter horizons were mainly attributed to weak dielectric contrasts amongst litter layers, with absolute differences in relative dielectric permittivity values often lower than 2 between humus horizons, and to uncertainties in the ground truth values. Radar signal inversions also provided reliable estimates of litter electromagnetic properties, with average relative dielectric permittivity values around 2.9 and 6.3 for OL and OF litters, respectively. These results are encouraging for the use of GPR for noninvasive characterization and mapping of forest litter. Perspectives for the application of the technique in biogeosciences are discussed.

1. Introduction

Forest litter is acknowledged to constitute a major component of forest ecosystems. Indeed, this layer, consisting essentially of shed vegetative parts and organic matter in various stages of decomposition at the soil surface, plays an important role in a series of ecosystem processes such as, notably, soil carbon sequestration [*Liski et al.*, 2006; *Jonard et al.*, 2007], nutrient storage and progressive release through decomposition [*Attiwill and Adams*, 1993; *Sayer*, 2006; *Jonard et al.*, 2009], soil water retention and dynamics [*Putuhena and Cordery*, 1996; *Tamai et al.*, 1998; *Gerrits et al.*, 2010; *Rasoulzadeh and Homapoor Ghoorabjiri*, 2014], buffering of soil temperature variations [*Sharratt*, 1997], tree regeneration [*Kostel-Hughes et al.*, 2005; *Barna*, 2011; *Cleavitt et al.*, 2011; *Pröll et al.*, 2015], and population dynamics of ground vegetation and soil fauna [*Ponge*, 2013]. Therefore, detailed characterization of litter horizons is required for proper understanding and modeling of ecosystem functioning and is furthermore essential in the actual context of global warming, litter being mainly composed of labile carbon and nutrient pools more sensitive to climate changes than the corresponding stocks in the mineral soil [*Conant et al.*, 2011; *Schmidt et al.*, 2011; *Erhagen et al.*, 2013; *Kruse et al.*, 2013]. Besides climate effect, forest litter thickness and composition are also influenced by stand characteristics (i.e., tree species and density) as well as by biological, soil and anthropogenic factors and may present strong spatial variability [*Yanai et al.*, 2003; *Jonard et al.*, 2006, 2008]. However, the methods traditionally used for litter and, by extension, humus (i.e., the part of the topsoil strongly influenced by biological activities and organic matter) characterization resorting to monolith or borehole sampling are labor intensive, time consuming, and disturbing or destructive. Furthermore, these conventional methods generally necessitate a large number of samples to capture the spatial variability of the property of interest [*Bednorz et al.*, 2000; *Bens et al.*, 2006]. In contrast, ground-penetrating radar (GPR) potentially allows for noninvasive and efficient characterization of organic layers with a high resolution over extended areas. Nevertheless, although GPR has been widely used

for more than two decades for the delineation of mineral and organomineral soil horizons and for the determination of their physical and hydrogeophysical properties [e.g., *Huisman et al.*, 2003; *Lambot et al.*, 2004; *Gerber et al.*, 2007, 2010; *Minet et al.*, 2011; *André et al.*, 2012; *Jonard et al.*, 2013] as well as for the investigation of peatland stratigraphy [e.g., *Proulx-McInnis et al.*, 2013; *Comas et al.*, 2015], the potential of this geophysical technique for forest humus characterization has been poorly examined so far. In a first study on this topic, *Winkelbauer et al.* [2011] surveyed the thickness of forest litter horizons using a time domain GPR device equipped with a 800 MHz center frequency antenna. They successfully retrieved the total thickness of humus horizons and could reconstruct its spatial variability but failed to delineate the different humus horizons. The simplifying hypotheses underlying the radar data processing method adopted by the authors and the analysis of the radar scans based on visual inspection and reflection pattern recognition partly explain their difficulty in delimiting humus horizons. Additional explanations are the limited radar range resolution given the rather low operating frequencies as well as the weak dielectric contrast between horizons and their relatively small thicknesses. More recently, *André et al.* [2015] used an ultrawideband (0.8–4 GHz) stepped-frequency continuous-wave (SFCW) GPR to evaluate the ability of the technique to provide detailed characterization of artificially reconstructed layers of three different beech litter types, defined according to their specification for the classification of forest humus forms [*Brethes et al.*, 1995; *Jabiol et al.*, 2013]: (i) recently fallen litter with original plant organs easily discernible to the naked eye (OL layer), (ii) fragmented litter in partial decomposition without entire plant organs (OF layer), and (iii) combination of OL and OF litter layers. Using full-wave inversion of the radar data [*Lambot et al.*, 2004; *Lambot and André*, 2014], these authors retrieved litter layer thicknesses with 1 cm accuracy and also obtained reliable estimates of litter electromagnetic properties (i.e., relative dielectric permittivity and frequency-dependent effective electrical conductivity).

In other respects, the presence of litter on the forest floor was found to significantly reduce the sensitivity of passive and active microwave remote sensing signals to the soil water content of forested areas [*Guglielmetti et al.*, 2008; *Grant et al.*, 2007; *Kurum et al.*, 2012; *Schwank et al.*, 2008; *Grant et al.*, 2009; *Rahmoune et al.*, 2014] or possibly to lead to inaccuracies and bias in the estimations of biophysical properties of forest canopies [*Wang et al.*, 1998; *Townsend*, 2002; *Roberts et al.*, 2007]. As a result, proper modeling of the forest backscatter requires litter in the radiative transfer models used to process microwave remote sensing data acquired over forests to be accounted for as well as having accurate knowledge of the radiative properties of this compartment and of their spatiotemporal variability [*Guglielmetti et al.*, 2008; *Grant et al.*, 2008, 2009; *Kurum et al.*, 2011]. However, although the potential detrimental effect of litter in accurately determining the parameter of interest is now well recognized and despite the research efforts undertaken over the past few years in that direction [e.g., *Della Vecchia et al.*, 2006, 2007; *Grant et al.*, 2008; *Guglielmetti et al.*, 2008; *Kurum et al.*, 2009; *Grant et al.*, 2010; *Rahmoune et al.*, 2013], *in situ* experiments related to this topic remain scarce. In this regard, GPR could also constitute a valuable tool allowing both detailed analysis of the influence of forest litter on radar data from proximal measurements [*André et al.*, 2015] and high-resolution mapping of litter constitutive properties with fine spatial and/or temporal resolutions. This information could then subsequently be used in remote sensing radiative transfer models.

Following the successful application of GPR by *André et al.* [2015] for the characterization of forest litter layers in controlled conditions, the objective of this study is to further investigate the ability of the technique to reconstruct litter horizons in undisturbed natural conditions. For that purpose, radar data were acquired *in situ* for contrasted litter types in forest stands of various tree species.

2. Material and Methods

2.1. Experimental Setup

The experiment was conducted on 19 June 2014 within the "Bois de Lauzelle," located near the town of Louvain-la-Neuve in central Belgium. GPR data and litter thickness reference measurements were collected at 21 locations every 5 m along a 100 m long transect, through stands of various deciduous and coniferous tree species, namely, pure western hemlock (*Tsuga heterophylla* (Raf.) Sarg.) stands, a mixed hemlock and common beech (*Fagus sylvatica* L.) stand, a clearing, a mixed deciduous stand with common beech, northern red oak (*Quercus rubra* L.) and pedunculate oak (*Quercus robur* L.), and a Norway spruce (*Picea abies* (L.) H. Karst) stand (Figure 1a). The transect was specially defined so as to cross a wide range of litter characteristics in terms of thickness and structure expected under the influence of the variations in species composition. The encountered humus types range from thin organic horizons in active decomposition (acidic mull) under the deciduous trees to thick accumulation of organic matter (moder) on the floor of the coniferous stands.

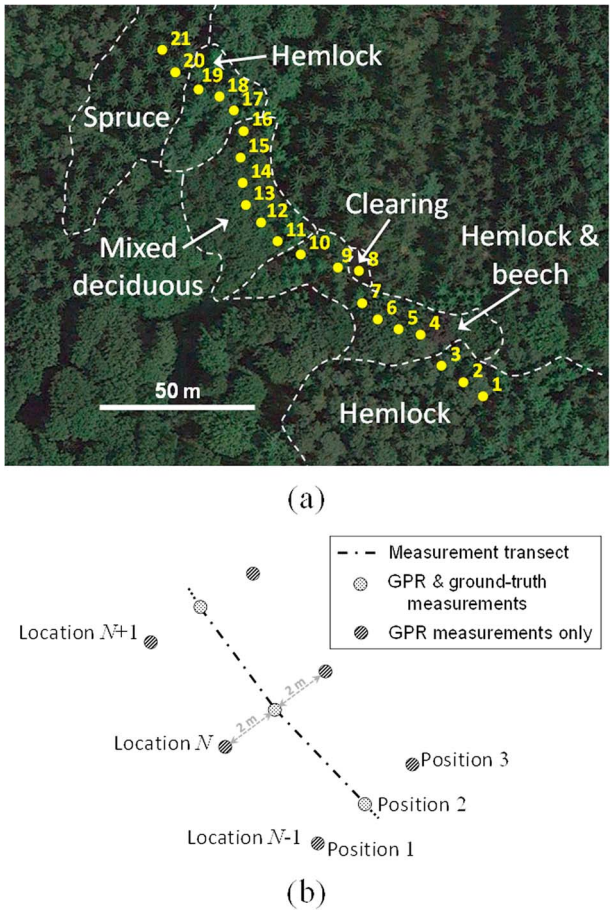

Figure 1. (a) Location of the measurement and sampling points. The dashed lines represent the limits of the crossed forest stands (modified from Google Earth). (b) Scheme of the measurement and sampling design at each location.

At each measurement location, GPR measurements were carried out at three different positions: a central measurement on the transect axis and two lateral measurements 2 m apart on each side, along a line perpendicular to the transect axis (Figure 1b). These pseudoreplicates aimed to capture the local spatial variability of litter thickness and physical properties around each measurement location under the influence of small-scale spatial variations of topography and environmental conditions. Furthermore, at each position, radar measurements were repeated twice so as to integrate measurement errors expected to result notably from small movements of the antenna held manually at about 30 cm above the litter surface during data acquisition. The antenna was held by the operator with arms stretched to avoid disturbing the litter within the antenna footprint during radar measurements. Subsequently to radar measurements, litter was characterized at the central position of each measurement location by monolith sampling using a square 0.09 m^2 area metal frame centered on the corresponding GPR measurement point. For each sampling point, the litter within the metal frame was integrally collected separating the OL and OF layers and was placed in hermetic plastic bags. Litter layer thicknesses were then measured to the nearest millimeter in the middle of each side of the sampling square, using a measuring tape. The middles of the square sides were chosen as references for litter layer thickness measurement as these points were the closest to the antenna footprint center. Following litter sample collections and ground truth measurements, litter was removed over wider areas (approximately 1.0 m × 1.0 m) centered on each sampling location and a second set of radar data was collected for characterizing the properties of the organomineral A horizon, which was considered as the bottom layer of the litter profile (i.e., the lower half-space of the electromagnetic model configuration).

Collected litter samples were brought to the laboratory for bulk density and volumetric water content determination. For this purpose, the volume of undisturbed (i.e., before sampling) litter was determined for each layer by multiplying the metal frame area by the average value of the corresponding four litter layer

thickness measurements carried out during sampling (see above). Each sample was weighted before and after oven drying at 105°C for 72 h. Litter bulk density was then calculated as the ratio between the sample dry mass and the corresponding undisturbed sample volume, while litter volumetric water content was computed by dividing the difference between the fresh and dry weights by the undisturbed sample volume.

2.2. Radar Measurements

The radar system used in this study is identical to that adopted for the controlled experiment. It consisted of an ultrawideband SFCW radar connected to a transmitting and receiving doubled-ridge horn antenna (BBHA 9120 A, Schwarzbeck Mess-Elektronik, Schönau, Germany) with 14×24 cm^2 aperture area and 22 cm height. The antenna nominal frequency range is 0.8 to 5.2 GHz, and its isotropic gain ranges from 4.4 to 14.0 dBi. It was connected to the reflection port of a vector network analyzer (VNA, ZVL, Rohde & Schwarz, Munich, Germany) with a high-quality N-type 50 Ω coaxial cable. The VNA was calibrated at the connection between the coaxial cable and the antenna using a standard Open-Short-Match calibration kit. The frequency-dependent complex ratio $S_{11}(f)$ between the returned and the emitted signals was measured sequentially at 734 evenly stepped frequencies from 0.8 to 5.2 GHz with a frequency step of 6 MHz, f being the frequency. The use of a frequency domain radar was preferred to that of a pulse radar for its generally higher signal-to-noise ratio. Furthermore, time domain GPR systems generally present a more limited bandwidth and generally suffer from significant drift. Hence, the frequency domain radar permits both a better range resolution and the consideration of frequency dependence of medium electromagnetic properties (see below). Finally, in contrast to classical GPR systems, the physical quantity measured by the VNA is exactly known and is defined as an international standard, which is more suitable to full-wave modeling and inversion of the GPR signal.

2.3. Radar Data Processing

2.3.1. Radar Model

Identically to the controlled experiment [*André et al.*, 2015], the measured radar signal was modeled using the far-field radar equation introduced by *Lambot et al.* [2004], formulated in the frequency domain as follows:

$$S_{11}(f) = \frac{b(f)}{a(f)} = R_0(f) + \frac{T(f)G_{xx}^{\uparrow}(f)}{1 - G_{xx}^{\uparrow}(f)R_s(f)} \tag{1}$$

where $S_{11}(f)$ is the measured complex ratio between the backscattered $b(f)$ and the incident $a(f)$ fields at the VNA reference plane, $R_0(f)$, $T(f)$ and $R_s(f)$ are antenna transfer functions characterizing the antenna radiative properties, and $G_{xx}^{\uparrow}(f)$ is a Green's function representing the response of the air-subsurface system and is formulated as an exact solution of the 3-D Maxwell's equations for electromagnetic waves propagating in planar layered media. A local plane wave field distribution of the backscattered field over the antenna aperture is assumed in this model, which holds when the height of the antenna above the planar layered medium is larger than 1.2 times the largest dimension of its aperture [*Tran et al.*, 2013]. The antenna transfer functions are determined from radar measurements over well-characterized medium configurations for which the corresponding Green's functions can be computed [*Lambot et al.*, 2004, 2006a].

Rearranging equation (1), it is possible to filter the antenna effects out of the raw radar data and obtain in this way the observed Green's function $G_{xx}^{\uparrow \mathrm{meas}}(f)$ corresponding to the medium response only:

$$G_{xx}^{\uparrow \mathrm{meas}}(f) = \frac{S_{11}(f) - R_0(f)}{S_{11}(f)R_s(f) + T(f) - R_0(f)R_s(f)} \tag{2}$$

2.3.2. Model Configurations

The GPR data acquired after litter removal were processed considering a two-layer electromagnetic model in order to characterize the A horizon (Figure 2a). The first layer represents the air layer between the antenna and the soil surface. Its electrical conductivity and relative dielectric permittivity values were set to the theoretical values $\sigma_0 = 0$ Sm^{-1} and $\varepsilon_{r,0} = 1$, respectively, and its thickness corresponds to the sum of the distance between the antenna phase center and its aperture (pc) with the antenna height (h_0). The second layer is the lower half-space and represents the A horizon. Its electrical conductivity was set to $\sigma_1 = 0$ S m^{-1}, referring to the findings of *Lambot et al.* [2006b]. Accordingly, the corresponding radar data were inverted for h_0 and A horizon relative dielectric permittivity ($\varepsilon_{r,A}$) focusing on the surface reflection (see section 2.3.3).

The GPR data collected in the presence of litter were analyzed using a four-layer model (Figure 2b). As for the previous configuration, the first layer corresponds to the air layer between the antenna phase center and the

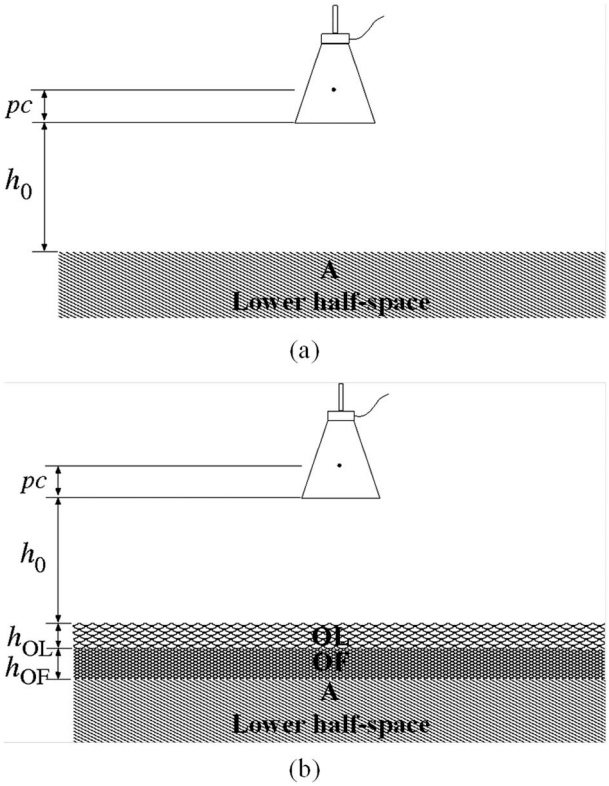

Figure 2. Schemes of the electromagnetic model configurations considered to process GPR data collected (a) after litter removal and (b) in the presence of litter.

litter surface and the lower half-space represents the A horizon, the relative dielectric permittivity of which was set to the value retrieved from inversion of the signal measured after litter removal. The second and the third layers correspond to the OL and OF litter layers, respectively. As highlighted in the controlled experiment [*André et al.*, 2015], proper modeling of the radar signal acquired above litter requires frequency dependence of medium properties to be considered in order to account for both relaxation and scattering phenomena. Based on the results of the previous experiment, the frequency dependence of litter dielectric permittivity was assumed to be negligible, while the frequency dependence of effective electrical conductivity was described by the following linear equation:

$$\sigma(f) = \sigma_{0.8\mathrm{GHz}} + a(f - 0.8 \times 10^9) \tag{3}$$

where $\sigma_{0.8\mathrm{GHz}}$ is the reference electrical conductivity at 0.8 GHz and a is the linear variation rate of $\sigma(f)$. Furthermore, as evidenced by the findings of the controlled experiment, $\sigma_{0.8\mathrm{GHz}}$ was considered as equal to 0 S m^{-1}.

In all cases, the magnetic permeability μ of each layer was assumed as equal to that of free space (i.e., $\mu_0 = 4\pi \times 10^{-7}$ H m^{-1}), which holds for nonmagnetic materials as found in litter and soils in most unpolluted environments [e.g., *Matysek et al.*, 2008; *Magiera et al.*, 2015].

2.3.3. Model Inversion

As mentioned above, inversion of radar data acquired after litter removal for estimation of parameter $\varepsilon_{r,A}$ was carried out in the time domain by focusing on the surface reflection, adopting the approach proposed by *Lambot et al.* [2006b]. In contrast, full-wave inversion of GPR data collected above litter was performed in the frequency domain to determine the electromagnetic properties and the thicknesses of the litter layers (i.e., $\varepsilon_{r,OL}$, $\varepsilon_{r,OF}$, a_{OL}, a_{OF}, h_{OL}, and h_{OF}). Besides, a simplified model was also tested by neglecting a_{OF}, in order to investigate the relevance of accounting for the frequency dependence of the effective electrical conductivity of the second litter layer as well as to reduce the number of unknowns. In all cases, optimized parameters were estimated through a least squares inverse problem by minimizing an objective function expressed as the sum of squares of the amplitudes of the differences between the measured and the modeled Green's functions.

We refer to *André et al.* [2015] for a more detailed description of the considered model configurations and optimization procedure.

2.4. Statistics

Statistical tests and measures of agreement were carried out in addition to graphical comparisons in order to examine the correspondence between estimated and measured values of litter layer thicknesses. Statistical tests consisted in a paired Student's *t* test and in a linear regression between two sets of values, and the selected measures of agreement were the Pearson's correlation coefficient (*r*), the root-mean-square error (RMSE), and the fractional bias (FB) defined as follows by *Janssen and Heuberger* [1995]:

$$\mathrm{FB} = \frac{\overline{E} - \overline{M}}{1/2(\overline{E} + \overline{M})} \tag{4}$$

where $\overline{E}$ and $\overline{M}$ are, respectively, the means of the estimated and measured values of the considered parameter.

The paired Student's *t* test and FB quantify the bias between compared values. The regression analysis tests for the significance of the deviation of the intercept and of the slope from 0 and 1, respectively. Linear regression coefficients were determined through total least squares to account for the fact that both the dependent and the independent regression variables (i.e., the estimated and measured litter thicknesses) were associated with errors [*Markovsky and Van Huffel*, 2007]. Confidence intervals of regression coefficients were established using the bootstrap percentile method considering 10,000 replicated computations [*Efron and Tibshirani*, 1994]. Finally, the correlation coefficient quantifies the strength of the linear relationship between the two compared variables and the RMSE expresses the discrepancy between paired values.

3. Results and Discussion

3.1. Radar Signal Modeling

As stated above, the feasibility of characterizing litter using GPR was evaluated through inversion of the radar model (equation (1)) so as to estimate the litter layer constitutive properties. While data were collected over the 0.8 to 5.2 GHz frequency range, signal inversions were carried out between 0.8 and 2.2 GHz only due to noise appearing in the data at higher frequencies, presumably as a result of small movements of the antenna during the measurements and more complex scattering phenomena. Selected model fits for four contrasted situations along the measurement transect (i.e., pure hemlock stand, mixed hemlock-beech stand, clearing, and mixed deciduous stand) are shown in Figure 3 in the frequency and time domains, as representative of the fitting results obtained after inversion of the collected radar data. The measured Green's function as well as fits for both the complete and the simplified model versions are presented on each graph.

In each case, relatively good correspondence is found between measured and modeled Green's functions, whatever the model version. The signal phase in the frequency domain and, therefore, the propagation time in the time domain are systematically well reproduced by the model. On the other hand, more noticeable discrepancies are sometimes observed between the amplitudes of the measured and modeled Green's functions. These observations prevail particularly for the frequency domain, while, in the time domain, the major signal reflections are generally properly described by the models and differences between measured and modeled signals primarily occur at larger propagation times, corresponding mainly to the lower half-space.

The generally similar fits observed for both model versions suggests that considering frequency dependence of the OF layer effective electrical conductivity via parameter a_{OF} is not necessary. This statement will be further investigated below when examining the inversion results.

3.2. GPR Estimates of Litter Properties

3.2.1. Litter Layer Thicknesses

Figure 4 presents estimates of OL and OF litter layer thicknesses (h_{OL} and h_{OF}) and of total litter thickness ($h_{TOT} = h_{OL} + h_{OF}$) as a function of the corresponding measured values. Results are presented for both the complete and the simplified model versions and distinguishing the different stand compositions at the measurement locations. The corresponding statistics and measures of agreement are presented in Table 1 considering both the complete data set and a restricted data set for which the two points presenting extreme high measured values for h_{OL} and h_{TOT} in the mixed hemlock-beech stand were not considered to avoid

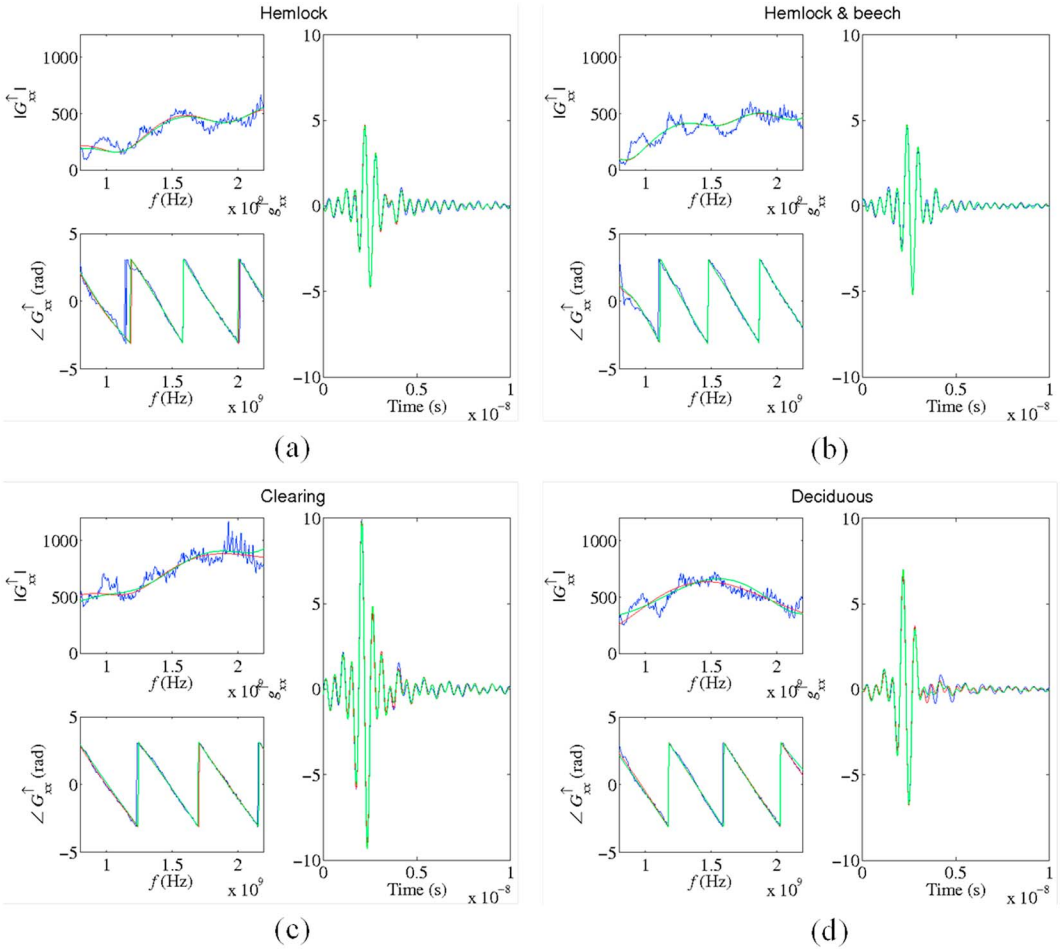

Figure 3. Measured (blue curves) and modeled Green's functions in the frequency and the time domains for four contrasted situations along the measurement transect: (a) litter of pure hemlock stand, (b) litter of mixed hemlock-beech stand, (c) litter in the clearing, and (d) litter of the mixed deciduous stand. The red and green curves represent the modeled Green's functions for the complete and the simplified versions of the model, respectively (i.e., with and without consideration of frequency dependence of litter effective electrical conductivity for the OF layer).

misinterpretation of the results due to the predominant influence of these two points on the statistics compared with the other observations. The predominance of these two points presenting very thick litter layer is particularly marked for the correlations between measured and estimated litter thicknesses, with generally much weaker correlation values and significance for the restricted data set compared with the complete one. In the following of this section, the results will be first analyzed based on the restricted data set and observations corresponding to the two extreme points will be then further examined and discussed.

The systematically nonsignificant t test results and very low FB values reveal the absence of bias for each comparison between estimates and measurements of litter layer thicknesses. Besides, RMSE values are around 1 cm for h_{OL} and around 2 cm for h_{OF} and h_{TOT}, which correspond to the RMSE value mentioned by *André et al.* [2015] for h_{OL} but are almost twice the values reported by these authors for h_{OF} and h_{TOT}. Yet in terms of correlation, better agreement is found between estimated and measured values for h_{OF} and h_{TOT} compared with h_{OL}. Indeed, focusing on the restricted data set in order to avoid the strong influence of the two extreme points, the correlation coefficients r between estimates and measurements amount to −0.01, 0.37, and 0.44 for h_{OL}, h_{OF}, and h_{TOT}, respectively, considering the complete model results. Corresponding values found for the simplified model are 0.14, 0.34, and 0.52 (Table 1). The very low correlations observed for h_{OL}, with largely nonsignificant P values of 0.971 and 0.578 for the complete and the simplified model versions, respectively, would at least partly arise from the much narrower range of values encountered for this parameter compared with that for h_{OF} and h_{TOT}. Indeed, as shown by the vertical and horizontal error bars representing 95% confidence intervals to average estimated and measured values, respectively, the range of values for h_{OL} is of the

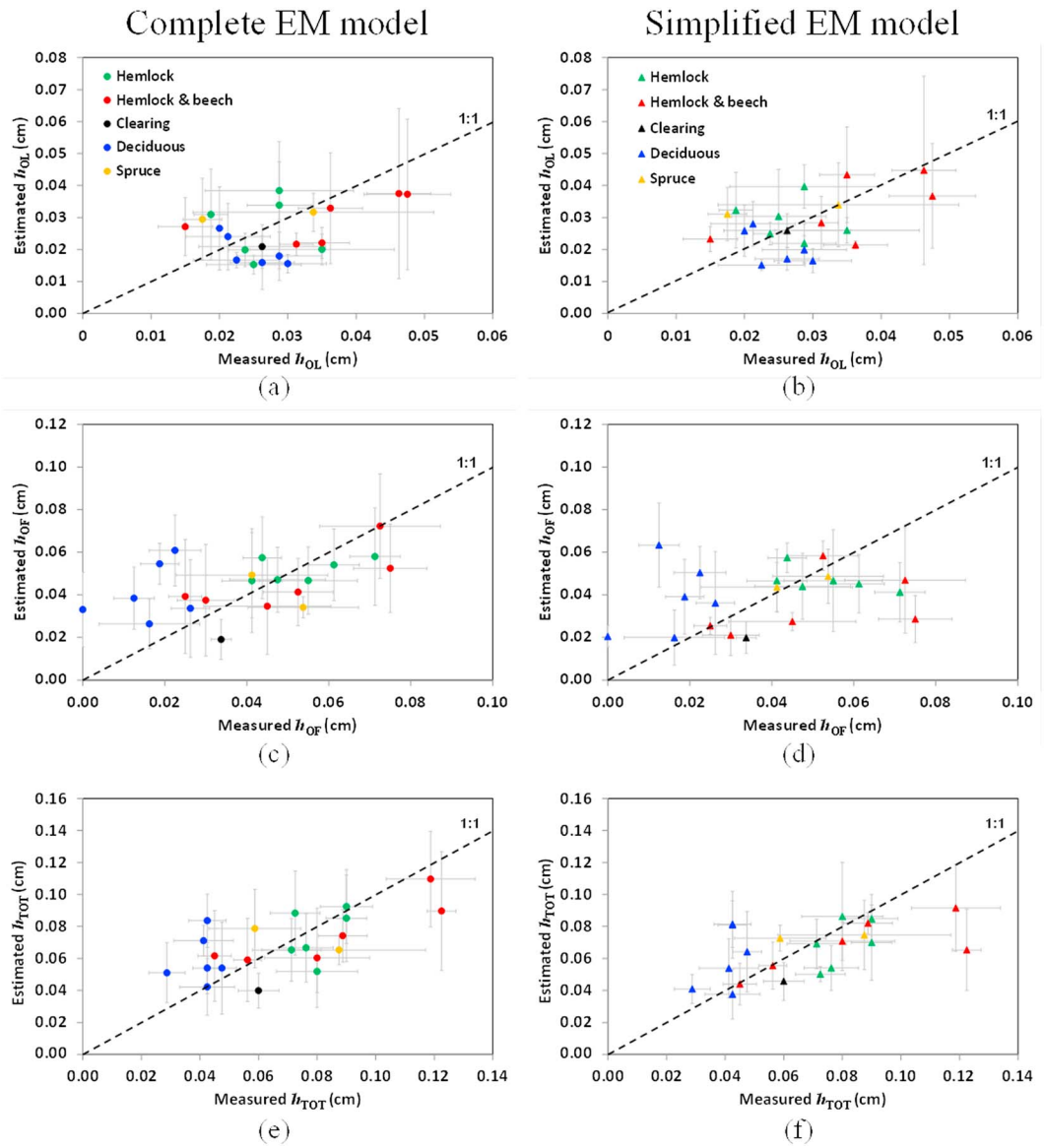

Figure 4. Comparison of inversion estimates for (a, b) OL litter layer thickness h_{OL}, for (c, d) OF litter layer thickness h_{OF}, and for (e, f) total litter thickness $h_{OL} + h_{OF}$ with corresponding measured values. Results are presented for both the complete (Figures 4a, 4c, and 4e) and the simplified (Figures 4b, 4d, and 4f) electromagnetic model versions. Symbol colors specify stand composition at each measurement location. Vertical and horizontal error bars represent 95% confidence intervals for the six estimated values and for the four measured values at each location, respectively. The dashed line is the 1:1 line.

same order of magnitude as its estimation and measurement errors (see Figures 4a and 4b). This also explains the nonsignificant values observed for the corresponding regression coefficients. Regarding h_{OF} (Figures 4c and 4d), the main discrepancies between estimates and measurements observed for both the complete and the simplified model versions are overestimations of the parameter occurring for its lowest measured values, corresponding to deciduous stand situations. In addition, for the simplified model, large underestimations are also found for the highest h_{OF} measured values, more particularly for one measurement point in the hemlock stand and for two points in the mixed hemlock-beech stand. Such observations give rise both to generally significant positive values observed for the intercept of the regressions and to slope coefficients significantly lower than 1. The smaller relative estimation and measurement errors observed for h_{OF} compared with h_{OL} provide larger correlations with values around 0.35, though these remain nonsignificant given the rather large discrepancies still present between h_{OF} estimations and measurements. The aforementioned discrepancies generally tend to attenuate for total litter thickness (Figures 4e and 4f) for which significant correlations

Table 1. Statistical Comparisons Between Measured and Inversely Estimated Litter Layer Thicknesses

		Paired *t* Test						Total Least Squares Regression			
	Parameter	*t* Ratio (*P* Value)		FB[a]	RMSE (m)[b]	r[c] (*P* Value)		Intercept [CI95][d]		Slope [CI95][d]	
					All Data						
Complete EM model	h_{OL}	−0.070	(0.945)	−0.0003	0.010	0.359	(0.110)	0.004	[−0.081;0.079]	0.76	[−2.13;3.80]
	h_{OF}	0.053	(0.958)	0.0007	0.018	0.510	(0.018)	0.028	[0.012;0.041]	0.41	[0.12;0.74]
	h_{TOT}	0.001	(0.999)	0.0000	0.019	0.641	(0.002)	0.029	[0.007;0.049]	0.59	[0.29;0.87]
Simplified EM model	h_{OL}	−0.013	(0.990)	−0.0001	0.009	0.441	(0.046)	0.001	[−0.076;0.041]	0.96	[−0.06;3.98]
	h_{OF}	−0.025	(0.980)	−0.0004	0.021	0.273	(0.232)	0.026	[0.007;0.051]	0.28	[−0.24;0.74]
	h_{TOT}	−0.032	(0.975)	−0.0008	0.022	0.533	(0.013)	0.035	[0.012;0.060]	0.45	[0.12;0.79]
					Restricted Data Set						
Complete EM model	h_{OL}	−0.055	(0.957)	−0.0002	0.010	−0.009	(0.971)	0.018	[−0.661;0.543]	0.01	[−4.43;6.08]
	h_{OF}	0.078	(0.939)	0.0010	0.018	0.371	(0.118)	0.031	[0.013;0.048]	0.33	[−0.11;0.72]
	h_{TOT}	0.028	(0.978)	0.0006	0.019	0.441	(0.048)	0.030	[−0.004;0.064]	0.56	[0.04;1.07]
Simplified EM model	h_{OL}	0.001	(0.999)	0.0000	0.009	0.136	(0.578)	−0.052	[−0.442;0.409]	2.94	[−15.45;18.71]
	h_{OF}	0.013	(0.990)	0.0002	0.019	0.336	(0.159)	0.021	[−0.005;0.057]	0.46	[−0.51;1.13]
	h_{TOT}	0.012	(0.991)	0.0002	0.017	0.524	(0.021)	0.023	[−0.001;0.058]	0.66	[0.18;1.00]

[a]Fractional bias (see equation (4)).
[b]Root-mean-square error.
[c]Pearson's correlation coefficient.
[d]95% confidence interval, established using the bootstrap percentile method (see section 2.4).

between measurements and estimates are found, revealing that the overestimations and underestimations observed for h_{OF} were partly associated with, respectively, underestimations and overestimations of h_{OL} at the corresponding measurement locations. This would indicate inaccurate delineation of these two horizons from GPR signal inversion in these cases, as also reported by *Winkelbauer et al.* [2011]. Yet although significant, these correlations remain relatively weak with values of 0.44 and 0.52 for the complete and simplified model versions, respectively, due to some large h_{TOT} overestimations that are still observed at some deciduous locations. These overestimations would then presumably arise from a weak contrast between litter and the A horizon at these locations. This statement is corroborated by the quite close values observed for the estimated dielectric permittivity of the two layers, notably in the deciduous stand (see Figure 5a). Similarly, low dielectric contrast would also partly explain underestimations of h_{TOT} for the two locations in the mixed hemlock-beech stand with the thickest litter layer. Nevertheless, in these latter cases, such observations could also result from the presence of large tree roots in the thick OF layer noticed during litter sampling at these points. Indeed, due to the presence of roots, which are detected as local anomalies by the radar, the actual medium configuration strongly diverges from that of a planar layered medium with homogeneous layers considered in the electromagnetic model, which would therefore affect the retrieval of litter layer thicknesses from radar data inversion. Furthermore, the closer correspondence observed between estimated and measured values for the complete model compared with the simplified model would arise from the fact that these roots induce radar signal scattering in the OF layer, which is better accounted for when considering frequency dependence of effective electrical conductivity for the OF layer in the model.

Considering these results, GPR appears to be a convenient tool to estimate total litter thickness (h_{TOT}) and retrieve its spatial variation with reasonable accuracy. In contrast, the ability of the technique to properly discriminate and accurately reconstruct individual litter horizons is more limited, in particular for the OL layer, given both the thinness of this horizon and its small thickness variations amongst the considered situations. As mentioned earlier, these observations partly arise from weak dielectric contrasts between horizons and better results are expected from data acquired during conditions increasing the contrast between layers. In this regard, performing radar measurements after some dry days, which follow a rainy period, would be advantageous as the upper layer would then be significantly drier than the lower one. In contrast, carrying out radar measurements after a prolonged dry period or, inversely, immediately after rain, is expected to be less favorable. Indeed, in the first case, the low water content along the layer profile would limit the contrast between horizons, while, in the second, the high water content of the superficial layer would induce the

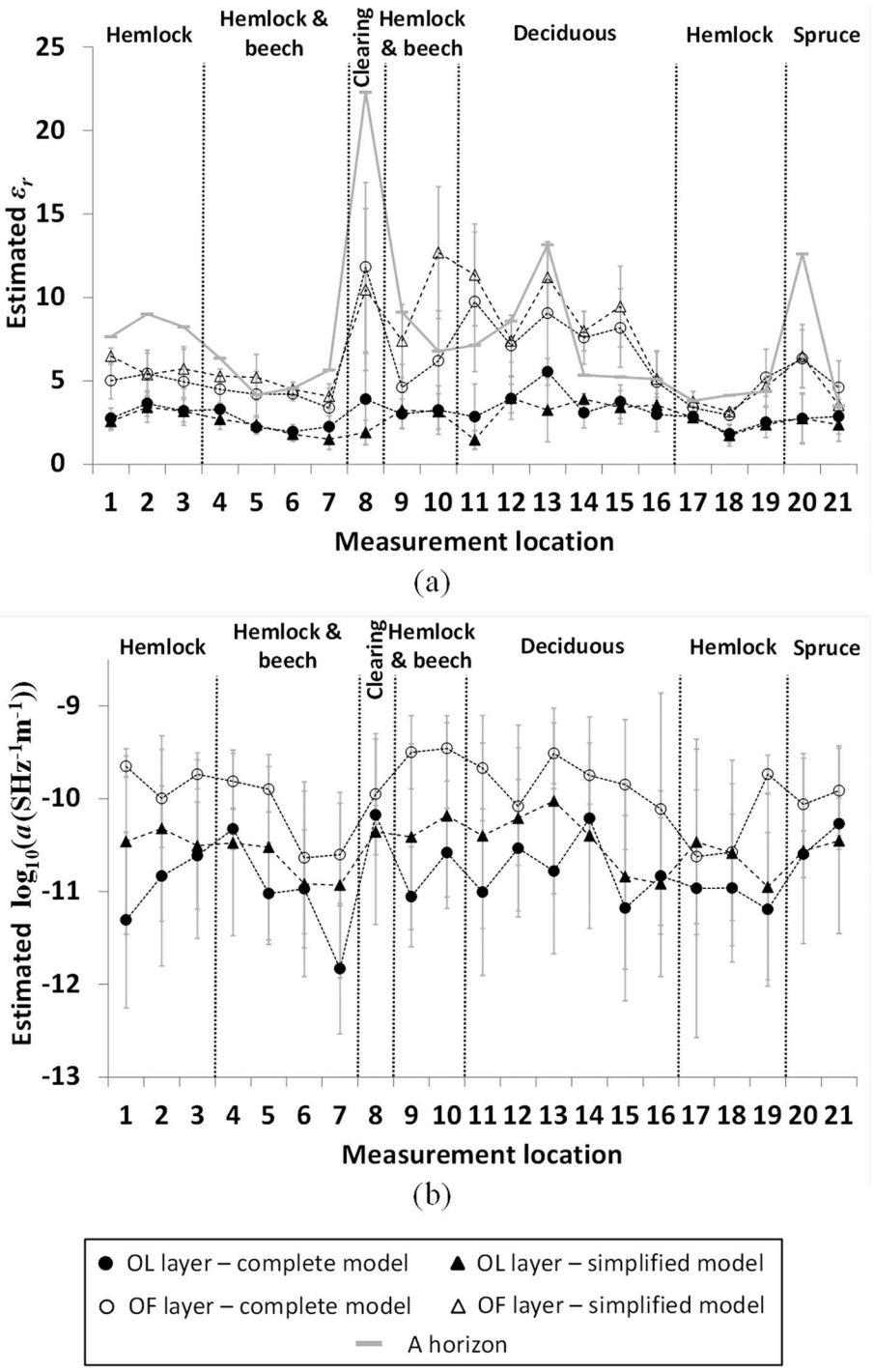

Figure 5. Variations of estimates (a) of the relative dielectric permittivity of the OL and OF litter layers ($\varepsilon_{r,\mathrm{OL}}$, $\varepsilon_{r,\mathrm{OF}}$), and of the A horizon ($\varepsilon_{r,\mathrm{A}}$) and (b) of the rate of variation of litter electrical conductivity with frequency ($\log_{10}(a)$) as a function of measurement location. Error bars represent 95% confidence intervals for the six estimated values at each location.

reflection of a large part of the incident signal at the litter surface, thereby limiting the transmission of the energy into the lower layers and reducing the signal-to-noise ratio. Besides, consideration of the presence of local objects such as roots or branches in the medium configuration of the electromagnetic model should also improve the quality of the results.

In other respects, it is worth noting that discrepancies between estimates and reference values also partly result from difficulties in the visual delimitation of these layers as well as from the local spatial variability of

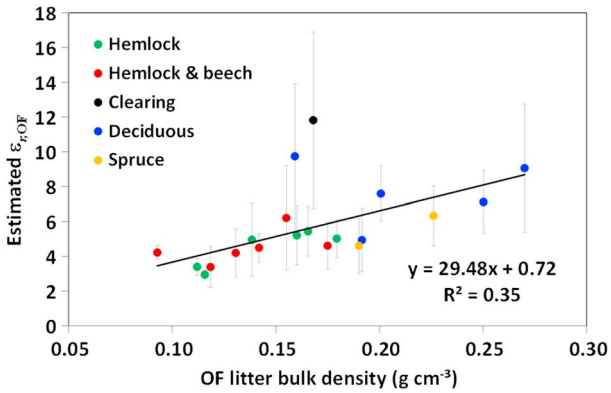

Figure 6. Variation of the estimates of the relative dielectric permittivity of the OF litter layer ($\varepsilon_{r,OF}$) as a function of OF litter bulk density. Error bars represent 95% confidence intervals for the six estimated values at each location.

their thicknesses at the sampling scale, leading inherently to inaccuracy of the ground truth measurements. This is particularly well illustrated by the large confidence intervals to the average measured thickness values represented by the horizontal error bars in Figure 4.

3.2.2. Litter Electromagnetic Properties

Figure 5 presents estimates of the relative dielectric permittivity (ε_r) and of the rate of variation of litter effective electrical conductivity with frequency ($\log_{10}(a)$) at each measurement location for the considered litter and soil horizons. Results are presented for both the complete and the simplified models.

Estimates of relative dielectric permittivity for the OL litter layer ($\varepsilon_{r,OL}$) are systematically lower than the corresponding values retrieved for the OF layer ($\varepsilon_{r,OF}$), with average values of 2.9 and 6.3, respectively (Figure 5a). However, the differences are not significant for all measurement locations. Such observations of higher values for $\varepsilon_{r,OL}$ compared with $\varepsilon_{r,OF}$ are consistent with findings of *André et al.* [2015]. Nevertheless, these authors reported lower values for both parameters, averaging around 1.3 and 3.9 for $\varepsilon_{r,OL}$ and $\varepsilon_{r,OF}$, respectively. Considering the strong positive correlations highlighted by several authors between relative dielectric permittivity and water content for litter and organic soils [*Topp et al.*, 1980; *DeRoo et al.*, 1991; *Roth et al.*, 1992; *Oleszczuk et al.*, 2004; *Pumpanen and Ilvesniemi*, 2005], contrasted litter layer water contents amongst both experiments are expected to partly explain these differences in their ε_r estimates. This explanation holds for the OL layer with a volumetric water content of 4.4% against the value of 1.4% for the controlled experiment. In contrast, it does not apply when comparing results for the OF layer, with opposite trends between average $\varepsilon_{r,OF}$ values and water content levels, amounting to 13.5% and 22.8% for the present and the controlled studies, respectively. Besides, no significant correlation between individual estimates of litter relative dielectric and litter water content measurements at the corresponding locations could be evidenced from our data, either for OL or for OF litter layers. In other respects, estimations of $\varepsilon_{r,OL}$ are in agreement with values reported in other works for litter and organic soils for similar water content [*DeRoo et al.*, 1991; *Roth et al.*, 1992; *Oleszczuk et al.*, 2004; *Pumpanen and Ilvesniemi*, 2005], while our estimates for $\varepsilon_{r,OF}$ are generally higher than these literature values. These differences may partly arise from the fact that these studies used time domain reflectometry (TDR), which may lead to inaccuracies in the determination of litter relative dielectric permittivity, notably if litter thickness is lower than the spatial sensitivity of the TDR probes [*Börner et al.*, 1996]. On the other hand, differences of litter dielectric permittivity amongst studies may also result from contrasted litter physical properties, other than water content. In this regard, a significant relationship could be established from our results between $\varepsilon_{r,OF}$ and OF litter bulk density (Figure 6). This relationship mainly arises from generally high values for both parameters in the deciduous stand and relatively low values for the mixed hemlock-beech and the pure hemlock stand. In contrast, such a relationship could not be established for the OL litter layer for which no particular trend is found for the variation of $\varepsilon_{r,OL}$ amongst the different locations along the transect (Figure 5a). Finally, whatever the layer, both model versions generally provide close estimates of litter dielectric permittivity.

Rates of variation of litter electrical conductivity with frequency (a) retrieved using the complete model are systematically higher for the OF layer compared with the OL layer, with values averaging to $10^{-9.9}$ S Hz^{-1} m^{-1} and to $10^{-10.8}$ S Hz^{-1} m^{-1}, respectively (Figure 5b). These agree quite well with corresponding values of

$10^{-10.6}$ S Hz^{-1} m^{-1} and $10^{-11.0}$ S Hz^{-1} m^{-1} reported by *André et al.* [2015]. Our approach of considering both scattering and dielectric losses through frequency dependence of litter effective electrical conductivity does not permit to determine the relative importance of each of these two phenomena in the considered litter layers. Nevertheless, scattering is expected to dominate for the OL layer given the heterogeneous nature and the surface roughness of this horizon consisting mainly of weakly decomposed plant organs. In contrast, the greater homogeneity of the OF layer combined with its higher water content would suggest that dielectric losses prevail in this horizon. Estimates of a_{OL} obtained from inversions using the simplified model by neglecting a_{OF} are generally higher than those provided by the complete model. This would indicate that in this case, a part of the electromagnetic phenomena considered through parameter a_{OF} in the complete model would be at least partly accounted for by parameter a_{OL} in the simplified model. Furthermore, as already mentioned, the generally quite limited differences observed in the results of both model versions not only with regard to model fitting but also concerning estimates of litter layer thicknesses and relative dielectric permittivities would indicate that parameter a_{OF} is not essential for proper modeling of the signal in most of the encountered cases and for the considered frequency range. The main differences among both models lie in the estimations of h_{OF} and h_{TOT} for points in the mixed hemlock-beech stand for which the presence of large roots in the OF layer was suspected to induce strong scattering which was considered through parameter a_{OF} in the complete model (see above). For all other locations, parameter a_{OL} appears to be sufficient to account for scattering and dielectric losses occurring in both layers. Moreover, discarding the two extreme points (i.e., considering the restricted data set), the agreement between estimated and measured litter thickness estimates is at least equivalent for both models or even better for the simplified model version than for the complete one (see Figure 4 and Table 1). In this regard, decreasing the number of parameters to be estimated from seven in the complete model to six in the simplified model allows the complexity of the inverse problem to be reduced, thereby leading to more stable parameter estimates.

3.3. Implications for Practical Applications of the Technique

The results of this exploratory study for *in situ* quantitative characterization of forest litter with GPR provide perspectives for practical applications in the field of biogeosciences.

A first application is the characterization of spatiotemporal variability of the forest floor carbon stocks. In this regard, the relationship established between $\varepsilon_{r,OF}$ and litter bulk density is particularly relevant. Indeed, combined with the estimate of litter layer thickness, GPR-derived litter bulk density would allow for the determination of litter biomass and, thereby, of carbon storage in this compartment. These estimations could be provided at the stand or plot scales from proximal radar data as in the present study. If acquired with sufficient spatial resolution, radar measurements would allow for efficient quantification of the spatial variability of litter carbon stocks, and repeated measurements over time would allow their temporal variations to be analyzed. Such data would constitute valuable information for the investigation of the processes generating litter carbon stock spatiotemporal patterns under the influence of variations of soil fertility and of stand density and species composition. In this way, GPR would help in assessing the relevance of forestry practices (e.g., choice of species, mixing of species, thinning and harvesting intensities, liming, and fertilization) with respect to forest floor carbon storage. This would provide insights for the definition of optimal forest management strategies adapted to global changes, carbon sequestration being one of the major contemporary roles attributed to forests. Finally, besides carbon, litter biomass determined from radar data would also permit to quantify nutrient pools in litter, if the associated nutrient concentrations are known.

Besides, airborne or spaceborne synthetic aperture radar (SAR) data are extensively used for the determination of biophysical properties of forest canopies, notably woody biomass [*Saatchi and Moghaddam*, 2000; *Saatchi et al.*, 2007; *Robinson et al.*, 2013]. However, litter is known to have a significant influence on the backscattered SAR signal and may induce inaccuracies and bias in the estimates of canopy parameters. As a result, litter constitutes a major component of the existing radiative transfer models used to process remote sensing radar data acquired over forested areas. In these models, litter is currently characterized through modeled or locally measured values of its radiative properties. However, inaccuracies, either in the modeling or in the measurement and spatial extrapolation of these properties, inherently lead to errors in the retrieval of the parameters of interest. In this respect, the determination of litter electromagnetic properties and of their spatial and/or temporal variability from proximal GPR data acquired over subzones of the area of interest could be used for improving remote sensing data products, either as direct input for the remote sensing models or as reference ground truth data for the calibration and the validation of the "litter module" of these

models. This would result in more robust forest woody biomass estimates which, combined with carbon or nutrient concentration data, would allow for large-scale assessment of tree carbon and nutrient contents.

The outcomes of these applications of litter characterization through GPR would provide essential information for detailed understanding and modeling of ecosystem functioning given the very large amounts of carbon and nutrients sequestered in the forest floor and tree biomass [*André and Ponette*, 2003; *Hart et al.*, 2003; *André et al.*, 2010; *Grüneberg et al.*, 2014; *De Vos et al.*, 2015]. Such information is especially important in the current context of global warming because of the sensitivity of carbon and nutrient cycles to climate changes. Nevertheless, despite the encouraging results of this first study for quantitative characterization of undisturbed forest litter with GPR, further research and validation are necessary before its routine application. In particular, a more physical description of the litter in the electromagnetic model, accounting for medium interface roughness [*Jonard et al.*, 2012] and considering the possible presence of local scatters such as roots, branches, and stones should notably help to improve the quality of the results.

4. Conclusions and Perspectives

In continuation of a previous controlled experiment [*André et al.*, 2015], this study evaluated the potential of GPR for *in situ* quantitative characterization of forest floor organic horizons in stands of various tree species. Ultrawideband (0.8–2.2 GHz) radar data were successfully reproduced by an electromagnetic model considering antenna effects and describing wave propagation in a three-dimensional layered medium using Green's functions. The model also accounted for dielectric losses and scattering phenomena occurring within litter through linear frequency dependence of litter effective electrical conductivity. Litter layer thicknesses and constitutive properties were retrieved through full-wave inversion of the GPR signal.

Though the agreement between estimated and reference layer thickness values was lower than that observed in controlled conditions, the results generally showed the ability of the technique to retrieve litter layer thicknesses with accuracies around 1 cm for the OL layer and around 2 cm for the OF and the total litter (i.e., OL + OF) horizons. Yet despite these reasonable accuracies, significant correlations between estimated and measured thicknesses were found for total litter only. This should be partly attributed to the low dielectric contrast between horizons for the litter water content conditions prevailing during data acquisition, as well as to the difficulty in the accurate visual separation of litter horizons during ground truth thickness measurements.

In other respects, reliable estimates of litter electromagnetic properties were obtained, with relative dielectric permittivity values averaging around 2.9 and around 6.3 for the OL and the OF litter layers, respectively. Moreover, a significant relationship was highlighted between relative dielectric permittivity and bulk density for OF litter. The combination of this relationship with litter layer thickness estimates would allow GPR to be used as a tool for quantifying litter biomass and, by extension, carbon and nutrient storage together with their spatial and/or temporal variations. Besides, another interesting perspective would be to resort to GPR data analysis and inversion to investigate the relationship between litter water content and its relative dielectric permittivity, which is of prime interest for the processing of remote sensing data over forests.

This study highlights the ability of GPR for the efficient and noninvasive characterization of forest litter, in contrast to the tedious and disturbing traditional methods used for humus description and sampling. The results show promising potential for the technique to provide valuable information for ecological and remote sensing studies concerned with forested areas. Future research in this direction will focus on the improvement of the radar electromagnetic model through a better physical description of litter medium, considering interface roughness and the possible presence of branches and roots in the litter horizons. Finally, investigations for the definition of optimal meteorological conditions preceding and during radar data acquisition causing significant variations in the dielectric permittivity over the litter profile and, thereby, permitting more accurate delineation of litter horizons through data inversion would also be of high interest.

Acknowledgments
This research was supported by the Fonds National de la Recherche Scientifique (FNRS, Belgium), the Université catholique de Louvain (UCL, Belgium), and Forschungszentrum Jülich GmbH (FZJ, Germany). We are grateful to the editorial board and two anonymous reviewers for their constructive comments and suggestions that helped to improve the previous version of this paper. Data and derived data products can be made available upon request to the authors.

References

André, F., and Q. Ponette (2003), Comparison of biomass and nutrient content between oak (Quercus petraea) and hornbeam (Carpinus betulus) trees in a coppice-with-standards stand in Chimay (Belgium), *Ann. Forest Sci.*, *60*(6), 489–502, doi:10.1051/forest:2003042.

André, F., M. Jonard, and Q. Ponette (2010), Biomass and nutrient content of sessile oak (Quercus petraea (Matt.) Liebl.) and beech (Fagus sylvatica L.) stem and branches in a mixed stand in southern Belgium, *Sci. Total Environ.*, *408*(11), 2285–2294, doi:10.1016/j.scitotenv.2010.02.040.

André, F., C. van Leeuwen, S. Saussez, R. Van Durmen, P. Bogaert, D. Moghadas, L. de Rességuier, B. Delvaux, H. Vereecken, and S. Lambot (2012), High-resolution imaging of a vineyard in south of France using ground penetrating radar, electromagnetic induction and electrical resistivity tomography, *J. Appl. Geophys.*, *78*, 113–122.

André, F., M. Jonard, and S. Lambot (2015), Non-invasive forest litter characterization using full-wave inversion of microwave radar data, *IEEE Trans. Geosci. Remote Sens.*, *53*(2), 828–840.

Attiwill, P. M., and M. A. Adams (1993), Nutrient cycling in forests, *New Phytol.*, *124*(4), 561–582.

Barna, M. (2011), Natural regeneration of Fagus sylvatica L: A review, *Austrian J. Forest Sci.*, *128*(2), 71–91.

Bednorz, F., M. Reichstein, G. Broll, F. K. Holtmeier, and W. Urfer (2000), Humus forms in the forest-alpine tundra ecotone at Stillberg (Dischmatal, Switzerland): Spatial heterogeneity and classification, *Arctic Antarctic Alpine Res.*, *32*(1), 21–29, doi:10.2307/1552406.

Bens, O., U. Buczko, S. Sieber, and R. F. Hüttl (2006), Spatial variability of O layer thickness and humus forms under different pine beech forest transformation stages in NE Germany, *J. Plant Nutr. Soil Sci.*, *169*(1), 5–15, doi:10.1002/jpln.200521734.

Börner, T., M. G. Johnson, P. T. Rygiewicz, D. T. Tingey, and G. D. Jarrell (1996), A two-probe method for measuring water content of thin forest floor litter layers using time domain reflectometry, *Soil Technol.*, *9*(3), 199–207.

Brethes, A., J. J. Brun, B. Jabiol, J. F. Ponge, and F. Toutain (1995), Classification of forest humus forms—A French proposal, *Ann. Forest Sci.*, *52*(6), 535–546, doi:10.1051/forest:19950602.

Cleavitt, N. L., T. J. Fahey, and J. J. Battles (2011), Regeneration ecology of sugar maple (Acer saccharum): Seedling survival in relation to nutrition, site factors, and damage by insects and pathogens, *Can. J. For. Res.*, *41*(2), 235–244.

Comas, X., N. Terry, L. Slater, M. Warren, R. Kolka, A. Kristiyono, N. Sudiana, D. Nurjaman, and T. Darusman (2015), Imaging tropical peatlands in Indonesia using Ground-Penetrating Radar (GPR) and Electrical Resistivity Imaging (ERI): Implications for carbon stock estimates and peat soil characterization, *Biogeosciences*, *12*(10), 2995–3007, doi:10.5194/bg-12-2995-2015.

Conant, R. T., et al. (2011), Temperature and soil organic matter decomposition rates—Synthesis of current knowledge and a way forward, *Global Change Biol.*, *17*(11), 3392–3404, doi:10.1111/j.1365-2486.2011.02496.x.

De Vos, B., N. Cools, H. Ilvesniemi, L. Vesterdal, E. Vanguelova, and S. Carnicelli (2015), Benchmark values for forest soil carbon stocks in Europe: Results from a large scale forest soil survey, *Geoderma*, *251-252*, 33–46, doi:10.1016/j.geoderma.2015.03.008.

Della Vecchia, A., K. Saleh, P. Ferrazzoli, L. Guerriero, and J. P. Wigneron (2006), Simulating L-band emission of coniferous forests using a discrete model and a detailed geometrical representation, *IEEE Geosci. Remote Sens. Lett.*, *3*(3), 364–368, doi:10.1109/lgrs.2006.873230.

Della Vecchia, A., P. Ferrazzoli, J. P. Wigneron, and J. P. Grant (2007), Modeling forest emissivity at L-band and a comparison with multitemporal measurements, *IEEE Geosci. Remote Sens. Lett.*, *4*(4), 508–512, doi:10.1109/lgrs.2007.900687.

DeRoo, R., Y. Kuga, M. C. Dobson, and F. T. Ulaby (1991), Bistatic radar scattering from organic debris of a forest floor, in *Remote Sensing: Global Monitoring for Earth Management. International Geoscience and Remote Sensing Symposium (IGARSS '91),* vol. I, pp. 15–18, IEEE, Helsinki, Finland, doi:10.1109/igarss.1991.577643.

Efron, B., and R. Tibshirani (1994), *An Introduction to the Bootstrap*, 456 pp., Taylor and Francis Ltd., United States.

Erhagen, B., M. Öquist, T. Sparrman, M. Haei, U. Ilstedt, M. Hedenström, J. Schleucher, and M. B. Nilsson (2013), Temperature response of litter and soil organic matter decomposition is determined by chemical composition of organic material, *Global Change Biol.*, *19*(12), 3858–3871, doi:10.1111/gcb.12342.

Gerber, R., C. Salat, A. Junge, and P. Felix-Henningsen (2007), GPR-based detection of Pleistocene periglacial slope deposits at a shallow-depth test site, *Geoderma*, *139*(3/4), 346–356.

Gerber, R., P. Felix-Henningsen, T. Behrens, and T. Scholten (2010), Applicability of ground-penetrating radar as a tool for nondestructive soil-depth mapping on Pleistocene periglacial slope deposits, *J. Plant Nutr. Soil Sci.*, *173*(2), 173–184, doi:10.1002/jpln.200800163.

Gerrits, A. M. J., L. Pfister, and H. H. G. Savenije (2010), Spatial and temporal variability of canopy and forest floor interception in a beech forest, *Hydrol. Process.*, *24*(21), 3011–3025.

Grant, J. P., J. P. Wigneron, A. A. Van de Griend, A. Kruszewski, S. S. Sobjaerg, and N. Skou (2007), A field experiment on microwave forest radiometry: L-band signal behaviour for varying conditions of surface wetness, *Remote Sens. Environ.*, *109*(1), 10–19, doi:10.1016/j.rse.2006.12.001.

Grant, J. P., K. Saleh-Contell, J. P. Wigneron, M. Guglielmetti, Y. H. Kerr, M. Schwank, N. Skou, and A. A. V. de Griend (2008), Calibration of the L-MEB model over a coniferous and a deciduous forest, *IEEE Trans. Geosci. Remote Sens.*, *46*(3), 808–818, doi:10.1109/tgrs.2007.914801.

Grant, J. P., A. A. Van de Griend, M. Schwank, and J. P. Wigneron (2009), Observations and modeling of a pine forest floor at L-band, *IEEE Trans. Geosci. Remote Sens.*, *47*(7), 2024–2034, doi:10.1109/tgrs.2008.2010252.

Grant, J. P., A. A. Van de Griend, J. P. Wigneron, K. Saleh, R. Panciera, and J. P. Walker (2010), Influence of forest cover fraction on L-band soil moisture retrievals from heterogeneous pixels using multi-angular observations, *Remote Sens. Environ.*, *114*(5), 1026–1037, doi:10.1016/j.rse.2009.12.016.

Grüneberg, E., D. Ziche, and N. Wellbrock (2014), Organic carbon stocks and sequestration rates of forest soils in Germany, *Global Change Biol.*, *20*(8), 2644–2662, doi:10.1111/gcb.12558.

Guglielmetti, M., M. Schwank, C. Maetzler, C. Oberdoerster, J. Vanderborght, and H. Fluehler (2008), FOSMEX: Forest soil moisture experiments with microwave radiometry, *IEEE Trans. Geosci. Remote Sens.*, *46*(3), 727–735, doi:10.1109/tgrs.2007.914797.

Hart, P. B. S., P. W. Clinton, R. B. Allen, A. H. Nordmeyer, and G. Evans (2003), Biomass and macro-nutrients (above- and below-ground) in a New Zealand beech (Nothofagus) forest ecosystem: Implications for carbon storage and sustainable forest management, *For. Ecol. Manage.*, *174*(1–3), 281–294, doi:10.1016/S0378-1127(02)00039-7.

Huisman, J. A., S. S. Hubbard, J. D. Redman, and A. P. Annan (2003), Measuring soil water content with ground penetrating radar: A review, *Vadose Zone J.*, *2*, 476–491.

Jabiol, B., A. Zanella, J. F. Ponge, G. Sartori, M. Englisch, B. van Delft, R. de Waal, and R. C. Le Bayon (2013), A proposal for including humus forms in the World Reference Base for Soil Resources (WRB-FAO), *Geoderma*, *192*, 286–294.

Janssen, P. H. M., and P. S. C. Heuberger (1995), Calibration of process-oriented models, *Ecol. Model.*, *83*(1–2), 55–66.

Jonard, F., L. Weihermüller, H. Vereecken, and S. Lambot (2012), Accounting for soil surface roughness in the inversion of ultrawideband off-ground GPR signal for soil moisture retrieval, *Geophysics*, *77*(1), H1–H7, doi:10.1190/geo2011-0054.1.

Jonard, F., M. Mahmoudzadeh, C. Roisin, L. Weihermüller, F. André, J. Minet, H. Vereecken, and S. Lambot (2013), Characterization of tillage effects on the spatial variation of soil properties using ground-penetrating radar and electromagnetic induction, *Geoderma*, *207–208*(1), 310–322, doi:10.1016/j.geoderma.2013.05.024.

Jonard, M., F. André, and Q. Ponette (2006), Modeling leaf dispersal in mixed hardwood forests using a ballistic approach, *Ecology*, *87*(9), 2306–2318.

Jonard, M., F. André, F. Jonard, N. Mouton, P. Proces, and Q. Ponette (2007), Soil carbon dioxide efflux in pure and mixed stands of oak and beech, *Ann. Forest Sci.*, *64*(2), 141–150, doi:10.1051/forest:2006098.

Jonard, M., F. André, and Q. Ponette (2008), Tree species mediated effects on leaf litter dynamics in pure and mixed stands of oak and beech, *Can. J. For. Res.*, *38*(3), 528–538, doi:10.1139/x07-183.

Jonard, M., L. Augusto, C. Morel, D. L. Achat, and E. Saur (2009), Forest floor contribution to phosphorus nutrition: Experimental data, *Ann. Forest Sci.*, *66*(5), 510, doi:10.1051/forest/2009039.

Kostel-Hughes, F., T. P. Young, and J. D. Wehr (2005), Effects of leaf litter depth on the emergence and seedling growth of deciduous forest tree species in relation to seed size, *J. Torrey Botanical Soc.*, *132*(1), 50–61.

Kruse, J., J. Simon, and H. Rennenberg (2013), Soil respiration and soil organic matter decomposition in response to climate change, in *Developments in Environmental Science*, vol. 13, pp. 131–149, Elsevier.

Kurum, M., R. H. Lang, P. E. O'Neill, A. T. Joseph, T. J. Jackson, and M. H. Cosh (2009), L-band radar estimation of forest attenuation for active/passive soil moisture inversion, *IEEE Trans. Geosci. Remote Sens.*, *47*(9), 3026–3040, doi:10.1109/tgrs.2009.2026641.

Kurum, M., R. H. Lang, P. E. O'Neill, A. T. Joseph, T. J. Jackson, and M. H. Cosh (2011), A first-order radiative transfer model for microwave radiometry of forest canopies at L-band, *IEEE Trans. Geosci. Remote Sens.*, *49*(9), 3167–3179, doi:10.1109/TGRS.2010.2091139.

Kurum, M., P. E. O'Neill, R. H. Lang, M. H. Cosh, A. T. Joseph, and T. J. Jackson (2012), Impact of conifer forest litter on microwave emission at L-band, *IEEE Trans. Geosci. Remote Sens.*, *50*(4), 1071–1084, doi:10.1109/tgrs.2011.2166272.

Lambot, S., and F. André (2014), Full-wave modeling of near-field radar data for planar layered media reconstruction, *IEEE Trans. Geosci. Remote Sens.*, *52*(5), 2295–2303, doi:10.1109/TGRS.2013.2259243.

Lambot, S., E. C. Slob, I. van den Bosch, B. Stockbroeckx, and M. Vanclooster (2004), Modeling of ground-penetrating radar for accurate characterization of subsurface electric properties, *IEEE Trans. Geosci. Remote Sens.*, *42*(11), 2555–2568, doi:10.1109/tgrs.2004.834800.

Lambot, S., M. Antoine, M. Vanclooster, and E. C. Slob (2006a), Effect of soil roughness on the inversion of off-ground monostatic GPR signal for noninvasive quantification of soil properties, *Water Resour. Res.*, *42*, W03403, doi:10.1029/2005WR004416.

Lambot, S., L. Weihermüller, J. A. Huisman, H. Vereecken, M. Vanclooster, and E. C. Slob (2006b), Analysis of air-launched ground-penetrating radar techniques to measure the soil surface water content, *Water Resour. Res.*, *42*, W11403, doi:10.1029/2006WR005097.

Liski, J., A. Lehtonen, T. Palosuo, M. Peltoniemi, T. Eggers, P. Muukkonen, and R. Makipaa (2006), Carbon accumulation in Finland's forests 1922-2004—An estimate obtained by combination of forest inventory data with modelling of biomass, litter and soil, *Ann. Forest Sci.*, *63*(7), 687–697, doi:10.1051/forest:2006049.

Magiera, T., H. Parzentny, L. Róg, R. Chybiorz, and M. Wawer (2015), Spatial variation of soil magnetic susceptibility in relation to different emission sources in southern Poland, *Geoderma*, *255–256*, 94–103, doi:10.1016/j.geoderma.2015.04.028.

Markovsky, I., and S. Van Huffel (2007), Overview of total least-squares methods, *Signal Process.*, *87*(10), 2283–2302.

Matysek, D., H. Raclavska, and K. Raclavsky (2008), Correlation between magnetic susceptibility and heavy metal concentrations in forest soils of the eastern Czech Republic, *J. Environ. Eng. Geophys.*, *13*(1), 13–26, doi:10.2113/JEEG13.1.13.

Minet, J., A. Wahyudi, P. Bogaert, M. Vanclooster, and S. Lambot (2011), Mapping shallow soil moisture profiles at the field scale using full-waveform inversion of ground penetrating radar data, *Geoderma*, *161*(3–4), 225–237, doi:10.1016/j.geoderma.2010.12.023.

Oleszczuk, R., T. Brandyk, T. Gnatowski, and J. Szatyłowicz (2004), Calibration of TDR for moisture determination in peat deposits, *Int. Agrophys.*, *18*(2), 145–151.

Ponge, J. F. (2013), Plant-soil feedbacks mediated by humus forms: A review, *Soil Biol. Biochem.*, *57*, 1048–1060, doi:10.1016/j.soilbio.2012.07.019.

Pröll, G., A. Darabant, G. Gratzer, and K. Katzensteiner (2015), Unfavourable microsites, competing vegetation and browsing restrict post-disturbance tree regeneration on extreme sites in the Northern Calcareous Alps, *Eur. J. Forest Res.*, *134*(2), 293–308, doi:10.1007/s10342-014-0851-1.

Proulx-McInnis, S., A. St-Hilaire, A. N. Rousseau, and S. Jutras (2013), A review of ground-penetrating radar studies related to peatland stratigraphy with a case study on the determination of peat thickness in a northern boreal fen in Quebec, Canada, *Progress Phys. Geogr.*, *37*(6), 767–786, doi:10.1177/0309133313501106.

Pumpanen, J., and H. Ilvesniemi (2005), Calibration of time domain reflectometry for forest soil humus layers, *Boreal Environ. Res.*, *10*, 589–595.

Putuhena, W. M., and I. Cordery (1996), Estimation of interception capacity of the forest floor, *J. Hydrol.*, *180*(1–4), 283–299.

Rahmoune, R., P. Ferrazzoli, Y. H. Kerr, and P. Richaume (2013), SMOS level 2 retrieval algorithm over forests: Description and generation of global maps, *IEEE J. Sel. Top. Appl. Earth Observations Remote Sens.*, *6*(3), 1430–1439, doi:10.1109/jstars.2013.2256339.

Rahmoune, R., P. Ferrazzoli, Y. K. Singh, Y. H. Kerr, P. Richaume, and A. Al Bitar (2014), SMOS retrieval results over forests: Comparisons with independent measurements, *IEEE J. Sel. Top. Appl. Earth Observations Remote Sens.*, *7*(9), 3858–3866.

Rasoulzadeh, A., and M. Homapoor Ghoorabjiri (2014), Comparing hydraulic properties of different forest floors, *Hydrol. Process.*, *28*(19), 5122–5130, doi:10.1002/hyp.10006.

Roberts, J. W., S. Tesfamichael, M. Gebreslasie, J. van Aardt, and F. B. Ahmed (2007), Forest structural assessment using remote sensing technologies: An overview of the current state of the art, *Southern Hemisphere Forest. J.*, *69*(3), 183–203, doi:10.2989/shfj.2007.69.3.8.358.

Robinson, C., S. Saatchi, M. Neumann, and T. Gillespie (2013), Impacts of spatial variability on aboveground biomass estimation from L-band radar in a temperate forest, *Remote Sens.*, *5*(3), 1001–1023, doi:10.3390/rs5031001.

Roth, C. H., M. A. Malicki, and R. Plagge (1992), Empirical evaluation of the relationship between soil dielectric constant and volumetric water content as the basis for calibrating soil moisture measurements by TDR, *J. Soil Sci.*, *43*(1), 1–13.

Saatchi, S., K. Halligan, D. G. Despain, and R. L. Crabtree (2007), Estimation of forest fuel load from radar remote sensing, *IEEE Trans. Geosci. Remote Sens.*, *45*(6), 1726–1740, doi:10.1109/tgrs.2006.887002.

Saatchi, S. S., and M. Moghaddam (2000), Estimation of crown and stem water content and biomass of boreal forest using polarimetric SAR imagery, *IEEE Trans. Geosci. Remote Sens.*, *38*(2), 697–709, doi:10.1109/36.841999.

Sayer, E. J. (2006), Using experimental manipulation to assess the roles of leaf litter in the functioning of forest ecosystems, *Biol. Rev.*, *81*(1), 1–31, doi:10.1017/s1464793105006846.

Schmidt, M. W. I., M. S. Torn, S. Abiven, T. Dittmar, G. Guggenberger, I. A. Janssens, M. Kleber, I. Kogel-Knabner, J. Lehmann, D. A. C. Manning, P. Nannipieri, D. P. Rasse, S. Weiner, and S. E. Trumbore (2011), Persistence of soil organic matter as an ecosystem property, *Nature*, *478*(7367), 49–56, doi:10.1038/nature10386.

Schwank, M., M. Guglielmetti, C. Matzler, and H. Fluhler (2008), Testing a new model for the L-band radiation of moist leaf litter, *IEEE Trans. Geosci. Remote Sens.*, *46*(7), 1982–1994, doi:10.1109/tgrs.2008.916983.

Sharratt, B. S. (1997), Thermal conductivity and water retention of a black spruce forest floor, *Soil Sci.*, *162*(8), 576–582.

Tamai, K., T. Abe, M. Araki, and H. Ito (1998), Radiation budget, soil heat flux and latent heat flux at the forest floor in warm, temperate mixed forest, *Hydrol. Process.*, *12*(13–14), 2105–2114.

Topp, G. C., J. L. Davis, and A. P. Annan (1980), Electromagnetic determination of soil water content: Measurements in coaxial transmission lines, *Water Resour. Res.*, *16*(3), 574–582.

Townsend, P. A. (2002), Estimating forest structure in wetlands using multitemporal SAR, *Remote Sens. Environ.*, *79*(2–3), 288–304, doi:10.1016/s0034-4257(01)00280-2.

Tran, A., F. André, C. Craeye, and S. Lambot (2013), Near-field or far-field full-wave ground penetrating radar modeling as a function of the antenna height above a planar layered medium, *Progress Electromagn. Res.*, *141*, 415–430.

Wang, Y., J. L. Day, and F. W. Davis (1998), Sensitivity of modeled C- and L-band radar backscatter to ground surface parameters in Loblolly pine forest, *Remote Sens. Environ.*, *66*(3), 331–342, doi:10.1016/S0034-4257(98)00074-1.

Winkelbauer, J., J. Volkel, M. Leopold, and N. Bernt (2011), Methods of surveying the thickness of humous horizons using Ground Penetrating Radar (GPR): An example from the Garmisch-Partenkirchen area of the Northern Alps, *Eur. J. Forest Res.*, *130*(5), 799–812, doi:10.1007/s10342-010-0472-2.

Yanai, R. D., S. V. Stehman, M. A. Arthur, C. E. Prescott, A. J. Friedland, T. G. Siccama, and D. Binkley (2003), Detecting change in forest floor carbon, *Soil Sci. Soc. Am. J.*, *67*(5), 1583–1593.